

Iron Porphyrin Carbenes as Catalytic Intermediates: Structures, Mössbauer and NMR Spectroscopic Properties, and Bonding**

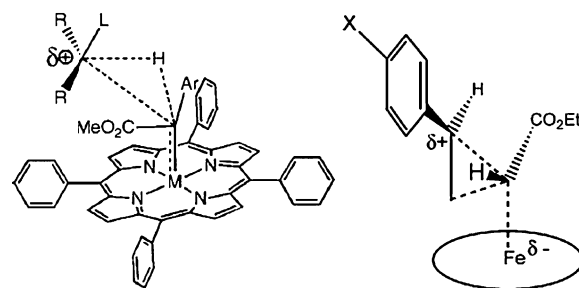
Rahul L. Khade, Wenchao Fan, Yan Ling, Liu Yang, Eric Oldfield, and Yong Zhang*

Abstract: Iron porphyrin carbenes (IPCs) are thought to be intermediates involved in the metabolism of various xenobiotics by cytochrome P450, as well as in chemical reactions catalyzed by metalloporphyrins and engineered P450s. While early work proposed IPCs to contain Fe^{II} , more recent work invokes a double-bond description of the iron–carbon bond, similar to that found in Fe^{IV} porphyrin oxenes. Reported herein is the first quantum chemical investigation of IPC Mössbauer and NMR spectroscopic properties, as well as their electronic structures, together with comparisons to ferrous heme proteins and an Fe^{IV} oxene model. The results provide the first accurate predictions of the experimental spectroscopic observables as well as the first theoretical explanation of their electrophilic nature, as deduced from experiment. The preferred resonance structure is $\text{Fe}^{\text{II}} \leftarrow \text{:C(X)Y}^0$ and not $\text{Fe}^{\text{IV}} = \text{C(X)Y}^{2-}$, a result that will facilitate research on IPC reactivities in various chemical and biochemical systems.

P450 cytochromes are a ubiquitous family of heme proteins, which act as catalysts for numerous biochemical reactions, and comprise high-valent ferryl species as important catalytic intermediates.^[1] Biomimetic P450 metalloporphyrin models have also been found to be efficient catalysts for a broad range of organic reactions, including C–H insertion, N–H insertion, cyclopropanation, as well as the olefination of aldehydes and ketones.^[2] The active species responsible for such reactivities have been proposed to be metalloporphyrin carbene complexes. In particular, iron porphyrin carbene (IPC) complexes have been shown to undergo several of these reactions, including C–H insertions and cyclopropanations.^[2f] IPC complexes were first observed several decades ago in the reactions of polyhalogenated methanes with porphyrins,^[3] reactions similar to those observed in the metabolism by cytochrome P450 of various xenobiotics, including toxic polyhalogenated compounds as well as diverse drugs.^[4]

More recently, engineered cytochrome P450s have been used in synthetically important reactions, such as carbene transfers, which are not observed in nature,^[2a] where IPC complexes are again thought to be key catalytic intermediates.

Given the broad general interest in IPCs in chemistry and biochemistry, it is surprising that the electronic structures and associated reactivities of IPC complexes are poorly understood. For instance, whether IPCs are best described as $\text{Fe}^{\text{II}} \leftarrow \text{:C(X)Y}^0$ or $\text{Fe}^{\text{IV}} = \text{C(X)Y}^{2-}$ (similar to $\text{Fe}^{\text{IV}} = \text{O}^{2-}$ in conventional P450 reactions), has not been resolved.^[2f,5] The presence of Fe^{II} was first proposed based on similarities of the UV/Vis and NMR spectra to those of diamagnetic Fe^{II} porphyrins,^[5c,d] and was also used in an early extended Hückel theory study,^[6] while in later work the presence of Fe^{IV} was proposed, based on similarities to the Mössbauer spectra of Fe^{IV} proteins and model systems.^[2f,5e] The double-bond feature of the iron–carbon bond in IPCs now seems generally accepted in the catalysis and biocatalysis areas,^[2a–c,f,h,5a] but has not, however, been investigated by ab initio quantum chemical methods. In addition, although IPCs were reported to effect electrophilic reactions by positive-charge build-up on the substrates (Scheme 1),^[2f,h,5a,7] there are no theoretical studies that explain this catalytic reactivity. Herein, we use density functional theory (DFT) calculations



Scheme 1. Experimentally proposed transition states in C–H insertion (left, Ref. [2h]) and cyclopropanation (right, Ref. [5a]) by IPCs.

to provide the first predictions of the Mössbauer and NMR spectroscopic observables of IPC complexes, as well as their geometries, and on the basis of these results, together with a detailed investigation of molecular orbitals and charges, we determined the origins of their reactivity. In particular, the preferred resonance structure was found to be quite different to that currently used in experimental studies of IPCs.

We initially calculated the Mössbauer spectra of IPCs since the ability to predict spectroscopic observables can reasonably be expected to give some confidence in the quality

[*] R. L. Khade, W. Fan, L. Yang, Prof. Dr. Y. Zhang
Department of Chemistry, Chemical Biology, and Biomedical
Engineering, Stevens Institute of Technology
Castle Point on Hudson, Hoboken, NJ 07030 (USA)
E-mail: yong.zhang@stevens.edu

Dr. Y. Ling
Department of Chemistry and Biochemistry, University of
Southern Mississippi, Hattiesburg, MS 39406 (USA)
Prof. Dr. E. Oldfield
Department of Chemistry, University of Illinois at
Urbana-Champaign, Urbana, IL 61801 (USA)

[**] This work was supported by an NSF grant (CHE-1300912) to Y.Z. and NIH grants (GM085774) to Y.Z. and (GM065307) to E.O.

Supporting information for this article is available on the WWW under <http://dx.doi.org/10.1002/anie.201402472>.

of the calculations and hence, confidence in other computed properties. We first used X-ray structures^[2f,5c] to compute the Mössbauer spectra of typical Fe^{IV} and Fe^{II} complexes, **1** and **2**, respectively (Figure 1). The compound **1** contains an Fe=O bond and is currently the only Fe^{IV} complex with a reported X-ray structure,^[8] whereas the heme site in carbomonoxy-myoglobin (MbCO) is known to possess an Fe^{II} center.^[9] We

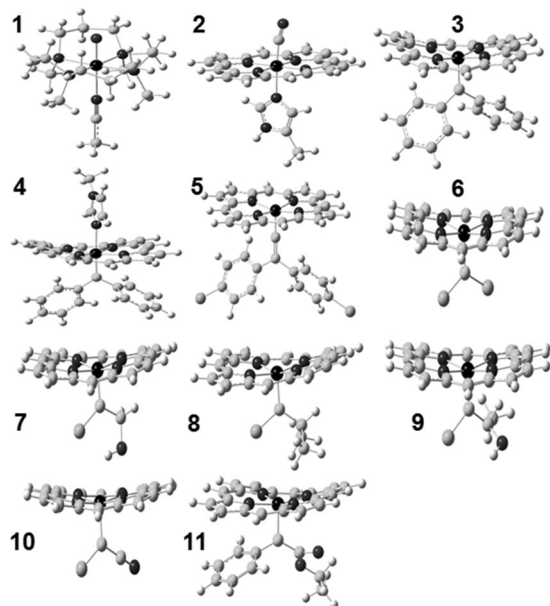


Figure 1. Molecular models used in this work for [Fe^{IV}(O)(TMC)(NCCH₃)²⁺ (**1**), MbCO active site (**2**), [Fe(TPFPP)(CPh₂) (**3**), [Fe(TPFPP)(CPh₂)(Melm)] (**4**), [Fe(TPP){C=C(C₆H₄Cl)₂} (**5**), [Fe(TPP)(CCl₂) (**6**), [Fe(TPP){CCl(CH₂OH)} (**7**), [Fe(TPP){CCl(CHMe₂)} (**8**), [Fe(TPP){CCl(CHMe(OH))} (**9**), [Fe(TPP)(CClCN)] (**10**), [Fe(TPFPP){C(Ph)CO₂Et}] (**11**). TMC = 1,4,8,11-tetramethyl-1,4,8,11-tetraazacyclotetradecane, Melm = *N*-methylimidazole, TPFPP = *meso*-tetraakis(pentafluorophenyl)porphyrinato dianion, TPP = *meso*-tetraphenylporphyrinato dianion.

used the DFT methods described previously, where they enabled excellent predictions of the Mössbauer isomer shift (δ_{Fe}) and quadrupole splitting (ΔE_{Q}) values in more than 50 iron proteins and model systems encompassing the most common iron spin ($S = 0, 1/2, 1, 3/2, 2, 5/2$), oxidation (Fe⁰, Fe^{II}, Fe^{III}, Fe^{IV}, Fe^{VI}), and coordination (2,3,4,5,6) states^[10] (see the Supporting Information for computational details of the methods used here).

We first calculated the Mössbauer properties of **1** and **2** with all possible spin states and also evaluated the relative stability of other spin states with respect to the singlet state ($\Delta E_{S=0}$). As shown in Table 1, the calculations correctly reproduced the experimental ground states of a triplet for **1** and a singlet for **2**,^[8,9b] and only computed results obtained by using experimental spin states produced good predictions of both Mössbauer parameters, thus providing confidence in the methods used. We then investigated the IPCs **3–5** (Figure 1), intermediates in catalysis and the degradation of polyhalogenated compounds. All porphyrin *meso* substituents were replaced with hydrogen atoms to facilitate calcu-

Table 1: Mössbauer properties of Fe^{IV}, Fe^{II}, and IPC complexes.

System	<i>S</i>	δ_{Fe} [mm s ⁻¹]	ΔE_{Q} [mm s ⁻¹]	$\Delta E_{S=0}$ [kcal mol ⁻¹]
[Fe ^{IV} (O)(TMC)(NCCH ₃) ²⁺] 1	Expt ^[a]	1 0.17	1.24	
	Calc	0 0.11	-3.22	0.00
		1 0.13	1.25	-28.74
		2 0.097	0.53	-13.28
MbCO 2	Expt ^[b]	0 0.27	0.35	
	Calc	0 0.29	0.27	0.00
		1 0.38	0.33	30.99
		2 0.48	2.87	58.40
[Fe(TPFPP)(CPh ₂)] 3	Expt ^[c]	0 0.03	(-)-2.34	
	Calc	0 0.10	-2.37	0.00
		1 0.053	-2.97	20.61
		2 0.056	-2.90	69.16

[a] Ref. [8]. [b] Ref. [9b]. [c] Ref. [2f]. The sign was not determined experimentally.

lations. The compound **3** is the only known IPC characterized by both X-ray crystallography and Mössbauer spectroscopy and the DFT results again reproduced the known singlet ground state, thus providing good agreement between both the experimental Mössbauer parameters and theory (Table 1). The predicted $\delta_{\text{Fe}}/\Delta E_{\text{Q}}$ values of 0.19/−1.76 mm s⁻¹ in **4** and 0.061/−1.94 mm s⁻¹ in **5** were similar to those obtained with **3**. So, overall, the Mössbauer isomer shifts in these IPC complexes are similar to the experimental results of about 0.09–0.22 mm s⁻¹ in nonporphyrin iron carbene complexes.^[11]

In contrast to the rather small range of δ_{Fe} values in IPCs, ΔE_{Q} values cover a larger range since ΔE_{Q} is related to the electric field gradient (EFG) tensor at the nucleus, which is more sensitive to the molecular environment than is δ_{Fe} .^[9b,10d,11] For instance, compared to the five-coordinate system **3**, the six-coordinate complex **4** has a smaller absolute ΔE_{Q} value because of increased symmetry and thus, a reduced EFG. It is of interest to note that the δ_{Fe} values in the IPCs are close to the experimental results of about 0.03–0.17 mm s⁻¹ for Fe^{IV} species,^[5e,12] which was previously used to support the presence of an Fe^{IV} feature in IPCs^[2f,5e] since in general, δ_{Fe} is a good indicator of the iron oxidation state.^[9b,10c] However, exceptions were found to result from strong ligand interactions,^[13] and some nonporphyrin iron carbenes have been reported to be Fe^{II} systems.^[11]

In contrast to δ_{Fe} results (which show similarities to Fe^{IV} systems), the relative stability of the spin states for the five-coordinate IPC complex **3** are the same as the typical Fe^{II} complex **2**, and are quite different to those found in the typical Fe^{IV} complex **1** (Table 1). The six-coordinate IPC complex **4** also exhibits the same trend with $\Delta E_{S=0}$ for the $S = 1$ state being 17.70 kcal mol⁻¹ higher, and for the $S = 2$ state, 41.18 kcal mol⁻¹ higher, thus indicating, again, similarities to Fe^{II} complexes.

To further investigate the Fe^{II}/Fe^{IV} bonding puzzle, we investigated the geometry-optimized structures of IPCs. Since there are no prior reports of this kind of study, we evaluated a number of DFT methods including the commonly used hybrid functional B3LYP and another hybrid functional, mPW1PW91, as well as the more recently developed func-

tionals M06, B97D, and ω B97XD, together with several basis sets (see the Supporting Information for details). The key geometric parameters of interest are those around the carbene center: the iron–carbene bond length R_{FeC} , the average iron and porphyrin–nitrogen bond length R_{FeN} , and the average length (R_{CC}) between the carbene carbon atom and its attached carbon atoms. The best predictions are shown in Table 2 and have only a 0.012 Å mean absolute deviation

Table 2: X-ray and computed geometric properties of IPCs.

System	S	R_{FeC} [Å]	R_{FeN} [Å]	R_{CC} [Å]
[Fe(TFPFP)(CPh ₂)(Melm)] 4	Expt ^[a]	0	1.827	1.973
	Calc	0	1.828	2.002
		1	2.018	1.993
		2	2.048	2.093
				1.458
[Fe(TFPFP){C(Ph) ₂ }] 3	Expt ^[a]	0	1.767	1.967
	Calc	0	1.764	1.991
		1	1.969	1.980
		2	2.030	2.112
				1.453
[Fe(TPP){C=C(C ₆ H ₄ Cl) ₂ }] 5	Expt ^[b]	0	1.690	1.985
	Calc	0	1.675	1.992
		1	1.751	2.050
		2	2.058	2.000
				1.489

[a] Ref. [2f]. [b] Ref. [5c].

(0.65 % mean percentage deviation) for the singlet ground state. In contrast, results from using higher spin states ($S=1$ and 2) have significantly larger errors, with 0.069 and 0.133 Å mean absolute deviations, respectively. These data further support the energy results discussed above, and are consistent with the experimental NMR assignment of a diamagnetic ground state.^[2f,5c,d]

We next investigated the ^{13}C NMR shifts/shieldings in a series of IPCs in detail. As shown in Table 3, experimental solution ^{13}C NMR chemical shifts of carbene carbon atoms encompass a broad range, from $\delta=210$ to 385 ppm downfield from TMS,^[2c,f,5d] and suggests that these NMR shifts may serve as sensitive probes of electronic structure. We used the geometry-optimized structures together with a series of DFT functionals and basis sets as well as the incorporation of solvent effects in the NMR chemical shielding calculations (see the Supporting Information for computational details). The best results are shown in Table 3. As shown in Figure 2 A, there is an excellent linear correlation between theory (σ^{calc})

Table 3: ^{13}C NMR chemical shifts/shieldings and charges.

	$\delta^{\text{expt}}_{\text{[a]}}$ [ppm]	$\sigma^{\text{calc}}(S=0)$ [ppm]	$\delta^{\text{pred}}(S=0)$ [ppm]	$\delta^{\text{pred}}(S=1)$ [ppm]	$\delta^{\text{pred}}(S=2)$ [ppm]	Q_{C} [e]
4	385.44	−198.88	380.27	2857.51	15 809.38	0.324
3	358.98	−178.38	349.57	800.64	9408.93	0.326
11	327.47	−163.06	326.61	1075.39	12 579.69	0.229
8	324.00	−165.80	330.73	22 695.04	23 522.84	0.275
9	312.00	−155.75	315.66	21 584.70	21 712.35	0.241
7	302.70	−155.77	315.69	21 592.17	28 689.45	0.200
6	224.70	−97.29	228.08	3421.81	74 530.39	0.053
10	210.00	−77.57	198.53	1386.70	51 894.04	0.056

[a] Refs. [2c,f,5d].

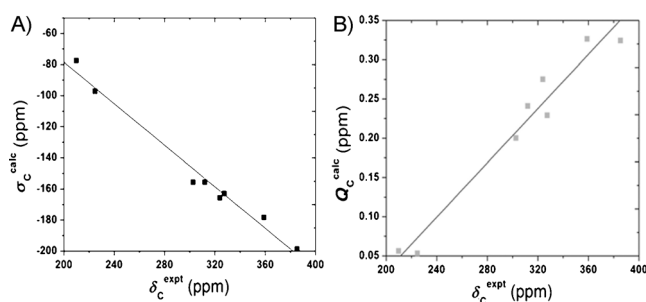


Figure 2. Plots of A) computed ^{13}C NMR chemical shieldings and B) charges versus experimental ^{13}C NMR chemical shifts in IPCs.

and experiment (δ^{expt}) for the singlet state, with the correlation coefficient $R^2=0.982$. The predicted shifts using this regression line (δ^{pred} s) yielded a 6.71 ppm mean absolute deviation (2.34 % mean percentage deviation), thus indicating that the broad range of ^{13}C NMR chemical shifts in IPCs is well reproduced in our quantum chemical calculations. In contrast, results from using $S=1$ or $S=2$ states yielded about 9000 and 30000 ppm mean absolute deviations, respectively, as a result of large hyperfine shifts (Table 3). These results provide strong additional evidence for a diamagnetic ground state in these IPC complexes, and are quite different to the paramagnetic states seen in Fe^{IV} species in heme/nonheme proteins and model systems.^[1,8,14] In addition, there were essentially no differences between the theory–experiment correlations when solvent effects were included ($R^2=0.980$) using the polarizable continuum method (see Table S6).

Given the success in predicting the spectroscopic observables, we next investigated the atomic charges of the carbene carbon atoms in the IPC systems. As shown in Table 3, these charges (Q_{C} values) cover a large range of about $0.3e$. The charges are all positive, with the charges in the known catalysts **3**, **4**, and **11** being particularly large, thus suggesting a physical basis for their electrophilic reactivity, as proposed experimentally (Scheme 1).^[2f,h,5a,7] A good correlation between these charges and the experimental NMR chemical shifts was also found, as illustrated in Figure 2 B ($R^2=0.958$), thus suggesting that ^{13}C NMR spectroscopy may be used as a probe of the reactivities of other IPC complexes.

The positive charges also suggest that the dominant feature in the metal–carbene bond involves carbene-to-metal donation. That is, carbenes with more electron-withdrawing substituents (e.g. CCl_2 as opposed to CPh_2) are associated with less positive charge (see Table 3), because electron-withdrawing substituents hinder the carbene's electron donation ability. These results thus support the importance of a $\text{Fe}^{\text{II}} \leftarrow \{\text{C}(\text{X})\text{Y}\}^0$ resonance structure over $\text{Fe}^{\text{IV}} = \{\text{C}(\text{X})\text{Y}\}^{2-}$ since the latter is associated with dominant metal-to-carbene back-donation, and thus partial negative charges on the carbene carbon atom, which is inconsistent with the electrophilic reactivities seen experimentally.

To further investigate the electronic structures of IPCs we examined the molecular orbitals (MOs) of the three IPC complexes having reported X-ray structures (**3–5**) and compared the MO results obtained with those of typical Fe^{IV} and Fe^{II} systems (**1,2**). Although the IPCs have different

structural features (five-coordinate, six-coordinate, as well as a vinylidene carbene), the electronic configurations of the frontier metal orbitals (FMOs) are the same: $(d_{xy})^2(d_{xz})^2-(d_{yz})^2(d_{z^2})^0(d_{x^2-y^2})^0$, as illustrated for **3** in the left-hand column of Figure 3. This is consistent with a d^6 Fe^{II} configuration, as

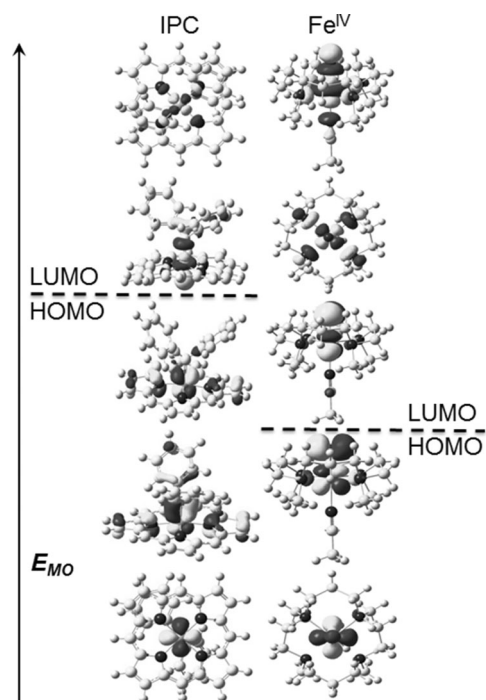


Figure 3. Frontier metal MO diagrams of the IPC complexes **3** (left) and **1** (right) with $S=0$.

found in the typical low-spin Fe^{II} system **2** reported previously,^[10c] and other noncatalyst IPC models.^[6] In contrast, as seen in the right-hand column in Figure 3 for the typical Fe^{IV} system **1** (in the $S=0$ state, to be more readily compared with the diamagnetic IPCs), the FMOs are $(d_{xy})^2(d_{xz})^2-(d_{yz})^2(d_{z^2})^0(d_{x^2-y^2})^0$, and are consistent with the expected d^4 Fe^{IV} configuration. This configuration has the same energy order as the FMOs in the triplet ground state, $(d_{xy})^2(d_{xz})^1-(d_{yz})^1(d_{x^2-y^2})^0(d_{z^2})^0$, as reported previously,^[15] and is clearly different to that seen in the IPC complexes. It is also interesting to note that compared to the two $\text{Fe} d\pi$ and $\text{O } p\pi$ interactions in the ground state of the Fe^{IV} complex **1**,^[15] there is only one $\text{Fe} d\pi$ and $\text{C } p\pi$ interaction in the ground state of **3**, as shown in Figure 3. The overlap-weighted natural atomic orbital bond order for $\text{Fe}-\text{O}$ in **1** is 0.797, which is approximately 50% larger than that (0.548) for $\text{Fe}-\text{C}$ in **3**, which is a further evidence for the difference between $\text{Fe}-\text{O}$ bonding in the Fe^{IV} system and $\text{Fe}-\text{C}$ bonding in the IPCs.

To further evaluate the possibility of the Fe^{IV} state in IPC complexes, calculations of **3** with a deliberate initial setup of Fe^{IV} and $(\text{CPh}_2)^{2-}$ and even with a different occupied $\text{Fe } 3d$ orbital sequence ($d_{xy} > d_{xz}/d_{yz}$) were performed. After convergence all systems yielded the same results as shown in Figure 3, which provides additional evidence that the Fe^{IV} state is not stable in these IPC complexes.

So, the MO results together with the charges, spin-state trends, and NMR shifts described above are all very similar to those found in Fe^{II} systems, rather than those seen in Fe^{IV} species. The predominant resonance structure is thus $\text{Fe}^{\text{II}} \leftarrow [\text{C}(\text{X})\text{Y}]^0$, which is quite different to the double-bond picture ($\text{Fe}^{\text{IV}} = [\text{C}(\text{X})\text{Y}]^{2-}$, analogous to $\text{Fe}^{\text{IV}} = \text{O}^{2-}$) used in much of the current literature,^[2a-c,f,h,5a] but is consistent with earlier spectroscopic suggestions^[5c,d] and their electrophilic reactivities.^[2f,h,5a,7] The less favorable Fe^{IV} state in IPC complexes as compared to $\text{Fe}^{\text{IV}} = \text{O}^{2-}$ intermediates is, however, reasonable, since carbon has a lower electronegativity than oxygen.

The results described above are of broad general interest since they represent the first successful predictions of the Mössbauer spectra (δ_{Fe} , ΔE_{O}), the ^{13}C NMR chemical shifts/shieldings as well as the local geometries of IPC complexes. They also provide the first theoretical basis for the origin of their electrophilic catalytic nature and also indicate that ^{13}C NMR spectroscopy may be a useful probe of IPC reactivity. Unlike the frequently used picture of a double bond between iron and carbon^[2a-c,f,h,5a] being analogous to the catalytic intermediates in conventional P450 reactions ($\text{Fe}^{\text{IV}} = \text{O}^{2-}$), IPC complexes are best described as involving $\text{Fe}^{\text{II}} \leftarrow [\text{C}(\text{X})\text{Y}]^0$, a result that should facilitate future studies of IPC systems in catalysis and in bioinorganic chemistry.

Received: February 18, 2014

Revised: April 8, 2014

Published online: June 6, 2014

Keywords: carbenes · iron · metalloenzymes · porphyrinoids · quantum chemistry

- [1] a) B. Meunier, S. P. de Visser, S. Shaik, *Chem. Rev.* **2004**, *104*, 3947–3980; b) R. Bernhardt, *J. Biotechnol.* **2006**, *124*, 128–145; c) S. P. de Visser, D. Kumar, S. Cohen, R. Shacham, S. Shaik, *J. Am. Chem. Soc.* **2004**, *126*, 8362–8363; d) P. Irigaray, D. Belpomme, *Carcinogenesis* **2010**, *31*, 135–148.
- [2] a) P. S. Coehlo, E. M. Brustad, A. Kannan, F. H. Arnold, *Science* **2013**, *339*, 307–310; b) C.-M. Che, V. K.-Y. Lo, C.-Y. Zhou, J.-S. Huang, *Chem. Soc. Rev.* **2011**, *40*, 1950–1975; c) C.-M. Che, C.-Y. Zhou, E. L.-M. Wong, *Top. Organomet. Chem.* **2011**, *33*, 111–138; d) H. Lu, W. I. Dzik, X. Xu, L. Wojtas, B. de Bruin, X. P. Zhang, *J. Am. Chem. Soc.* **2011**, *133*, 8518–8521; e) K. S. Chan, C. M. Lau, S. K. Yeung, T. H. Lai, *Organometallics* **2007**, *26*, 1981–1985; f) Y. Li, J. S. Huang, Z. Y. Zhou, C. M. Che, X. Z. You, *J. Am. Chem. Soc.* **2002**, *124*, 13185–13193; g) H. Y. Thu, G. S. M. Tong, J. S. Huang, S. L. F. Chan, Q. H. Deng, C. M. Che, *Angew. Chem.* **2008**, *120*, 9893–9897; *Angew. Chem. Int. Ed.* **2008**, *47*, 9747–9751; h) H. A. Mbuvi, L. K. Woo, *Organometallics* **2008**, *27*, 637–645; i) J.-C. Wang, Z.-J. Xu, Z. Guo, Q.-H. Deng, C.-Y. Zhou, X.-L. Wan, C.-M. Che, *Chem. Commun.* **2012**, *48*, 4299–4301; j) Y. Li, J. S. Huang, Z. Y. Zhou, C. M. Che, *J. Am. Chem. Soc.* **2001**, *123*, 4843–4844; k) Y. Chen, L. Y. Huang, X. P. Zhang, *Org. Lett.* **2003**, *5*, 2493–2496; l) L. K. Baumann, H. M. Mbuvi, G. Du, L. K. Woo, *Organometallics* **2007**, *26*, 3995–4002.
- [3] D. Mansuy, M. Lange, J. C. Chottard, P. Guerin, P. Morliere, D. Brault, M. Rougee, *J. Chem. Soc. Chem. Commun.* **1977**, 648–649.
- [4] a) G. Simonneaux, P. Le Maux, *Top. Organomet. Chem.* **2006**, *83–122*; b) R. Tolando, R. Ferrara, N. I. Eldirdiri, A. Albores,

- L. J. King, M. Manno, *Xenobiotica* **1996**, 26, 425–435; c) D. Mansuy, J. P. Battioni, J. C. Chottard, V. Ullrich, *J. Am. Chem. Soc.* **1979**, 101, 3971–3973; d) J. T. Groves, G. E. Avaria-Neisser, K. M. Fish, M. Imachi, R. L. Kuczkowski, *J. Am. Chem. Soc.* **1986**, 108, 3837–3838; e) P. Lafite, S. Dijols, D. C. Zeldin, P. M. Dansette, D. Mansuy, *Arch. Biochem. Biophys.* **2007**, 464, 155–168; f) N. Taxak, B. Patel, P. V. Bharatam, *Inorg. Chem.* **2013**, 52, 5097–5109.
- [5] a) T. S. Lai, F. Y. Chan, P. K. So, D. L. Ma, K. Y. Wong, C. M. Che, *Dalton Trans.* **2006**, 4845–4851; b) D. Mansuy, M. Lange, J. C. Chottard, J. F. Bartoli, B. Chevrier, R. Weiss, *Angew. Chem.* **1978**, 90, 828–829; *Angew. Chem. Int. Ed. Engl.* **1978**, 17, 781–782; c) D. Mansuy, J. P. Battioni, D. K. Lavalley, J. Fischer, R. Weiss, *Inorg. Chem.* **1988**, 27, 1052–1056; d) P. Guerin, J. P. Battioni, J. C. Chottard, D. Mansuy, *J. Organomet. Chem.* **1981**, 218, 201–209; e) D. R. English, D. N. Hendrickson, K. S. Suslick, *Inorg. Chem.* **1983**, 22, 367–368.
- [6] T. Tatsumi, R. Hoffmann, *Inorg. Chem.* **1981**, 20, 3771–3784.
- [7] J. R. Wolf, C. G. Hamaker, J. P. Djukic, T. Kodadek, L. K. Woo, *J. Am. Chem. Soc.* **1995**, 117, 9194–9199.
- [8] J. U. Rohde, J. H. In, M. H. Lim, W. W. Brennessel, M. R. Bukowski, A. Stubna, E. Munck, W. Nam, L. Que, *Science* **2003**, 299, 1037–1039.
- [9] a) G. S. Kachalova, A. N. Popov, H. D. Bartunik, *Science* **1999**, 284, 473–476; b) P. G. Debrunner in *Iron Porphyrins*, Vol. 3 (Eds.: A. B. P. Lever, H. B. Gray), VCH Publishers, New York, **1989**, pp. 139–234.
- [10] a) Y. Ling, Y. Zhang, *J. Am. Chem. Soc.* **2009**, 131, 6386–6388; b) J. Katigbak, Y. Zhang, *J. Phys. Chem. Lett.* **2012**, 3, 3503–3508; c) Y. Zhang, J. H. Mao, E. Oldfield, *J. Am. Chem. Soc.* **2002**, 124, 7829–7839; d) Y. Zhang, J. H. Mao, N. Godbout, E. Oldfield, *J. Am. Chem. Soc.* **2002**, 124, 13921–13930.
- [11] V. Guillaume, P. Thominot, F. Coat, A. Mari, C. Lapinte, *J. Organomet. Chem.* **1998**, 565, 75–80.
- [12] Y. Ling, V. L. Davidson, Y. Zhang, *J. Phys. Chem. Lett.* **2010**, 1, 2936–2939.
- [13] a) H. Andres, E. L. Bominaar, J. M. Smith, N. A. Eckert, P. L. Holland, E. Munck, *J. Am. Chem. Soc.* **2002**, 124, 3012–3025; b) F. M. MacDonnell, K. Ruhlandt-Senge, J. J. Ellison, R. H. Holm, P. P. Power, *Inorg. Chem.* **1995**, 34, 1815–1822; c) Y. Zhang, E. Oldfield, *J. Phys. Chem. B* **2003**, 107, 7180–7188.
- [14] a) M. Costas, M. P. Mehn, M. P. Jensen, L. Que, *Chem. Rev.* **2004**, 104, 939–986; b) A. Ikezaki, Y. Ohgo, M. Nakamura, *Coord. Chem. Rev.* **2009**, 253, 2056–2069.
- [15] Y. Zhang, E. Oldfield, *J. Am. Chem. Soc.* **2004**, 126, 4470–4471.